

EXAMINING EFFECTIVE EXPOSURE TIME AND BIOACCUMULATION RATE OF A SENSITIVE AND ACCURATE ACTIVE BIOMONITOR (*RAMALINA SINENSIS*) FOR ATMOSPHERIC SUSPENDED PARTICULATES

XU, P.^{1#} – MENG, J. W.^{2#} – ZHENG, X.^{1,3} – JIN, Q.² – WU, Q. F.¹ – WANG, L.² – LIU, A. Q.² – QIAO, S. F.² – XIA, Y.¹ – LIU, H. J.^{1*}

¹*School of Life Sciences, Institute of Life Science and Green Development, Hebei University, Baoding 071002, China*

(e-mail: pxu2000@163.com - Xu, P.; xx1441221708@163.com - Zheng, X.; wqf45@126.com - Wu, Q. F.; ayaxiayu@foxmail.com - Xia, Y.)

²*Hebei Key Laboratory of Mineral Resources and Ecological Environment Monitoring, Hebei Research Center for Geoanalysis, Baoding 071051, China*

(e-mail: mjw678@sina.com - Meng, J. W.; 13373121110@163.com - Jin, Q.; wanglei8812@163.com - Wang, L.; laq217510@sina.com - Liu, A. Q.; 1535722404@qq.com - Qia, S. F.)

³*Key Laboratory of Microbial Diversity Research and Application of Hebei Province, Research Center for Microbial Breeding and Conservation Engineering, Baoding, China*

[#]*These authors contributed equally*

^{*}*Corresponding author*

e-mail: liuhuaqie@hbu.edu.cn

(Received 11th Nov 2024; accepted 18th Mar 2025)

Abstract. *Ramalina sinensis* (*RSI*) is a good active biomonitor for atmospheric element deposition, but effective exposure time is yet unknown for this lichen. We transplanted *RSI* from a “clean” site to Tangshan, an industrially polluted city in China, during winter heating period. Three exposures time spans were used: two 2-month exposures (NJ2: Nov. 2016-Jan. 2017; JM2: Jan.-Mar. 2017) and one 4-month exposure (NM4: Nov. 2016-Mar. 2017). We measured concentrations of 47 elements. Exposed concentrations were higher than unexposed concentrations for almost all elements. Exposed to unexposed ratios (EU) and pollution load index at local scale (PLI_{site}) were greater in NM4 and NJ2 exposures than in JM2 exposure for 44 elements. Observed EU_{NM4} ratio was lower than expected for most elements. Pollution load index at regional scale (PLI_{zone}) had a NJ2:JM2 ratio similar to the average and cumulative daily mean concentrations of atmospheric suspended particulate matters (PMs). These results suggest that bioaccumulation primarily occurred within two months, indicating a retention time of less than two months and reaching an equilibrium by the end of this period. In conclusion, *RSI* is a sensitive and accurate active biomonitor for atmospheric suspended PMs, with an effective exposure time span of 2-4 months, during which *RSI* element concentrations vary proportionally to atmospheric suspended PMs.

Keywords: air pollution, biomonitoring, integration time, bioaccumulation rate, heavy metal, lichen

Introduction

Studying bioaccumulation of atmospheric contaminants/pollutants by lichens is a cost-effective method for assessing air quality (Garty, 2001; Brunialti and Frati, 2014; Abas, 2021). Lichens are symbiotic associations of fungi with cyanobacteria or green algae with distinct characteristics, such as slow growth, long lifetime, having wide intercellular spaces, relying highly on atmospheric nutrients, and tolerating air pollutants (Brunialti and Frati, 2014; Abas, 2021). These features allow them to accumulate airborne contaminants beyond their physiological requirements (Aprile et al., 2010; Osyczka et al., 2018). An increasing body of evidence shows a strong positive correlation between lichen and air metal concentrations, confirming their reliability as biomonitors of atmospheric elements (Loppi and Paoli, 2015; Massimi et al., 2019).

Active lichen biomonitoring is a widely used technique for assessing air quality. This technique involves transplanting lichen from a clean area to polluted areas and then comparing element concentrations before and after exposure. It helps assess levels, sources and trends of atmospheric contaminants/pollutants (Abas, 2021; Boonpeng et al., 2023; Lin et al., 2024). By providing adequate samples of a single lichen species across all monitoring sites, it minimizes the influence of species variability on lichen element concentrations. It also allows for flexible planning of monitor sites and exposure times (Abas, 2021). Moreover, it serves as a powerful tool to study the processes, mechanisms and factors that influence the bioaccumulation of atmospheric deposits in lichen thalli (Boonpeng et al., 2017; Zhao et al., 2019; Cecconi et al., 2021).

Ramalina sinensis Jatta (*RSI*) has been confirmed as a good active biomonitor (Tumur et al., 2011; Sohrabi et al., 2021; Li et al., 2024), but the sensitivity and accuracy of element bioaccumulation of this lichen in reflecting atmospheric deposition are yet unknown. Firstly, the effective exposure time span remains inadequately understood. Selecting the appropriate exposure time settings is critical for accurately assessing atmospheric element deposition using active biomonitoring, because exposure time has a pronounced influence on element bioaccumulation in lichen transplants (Garty, 2001; Brunialti and Frati, 2014). Retention time, also known as memory length, remembrance time or integration time, is a period during which the lichen transplants fail to effectively reflect element availability from the “new” environment and instead primarily reflect that from the “old” environment (Reis et al., 1999; Godinho et al., 2008; Zhao et al., 2019; Jia et al., 2020). A shorter retention time typically indicates a higher sensitivity of lichen bioaccumulation to changes in elemental availability within the environment. Conversely, prolonged exposure times may lead to a decoupling of element concentrations between lichen and atmosphere, thus reducing the accuracy of lichen element concentrations in reflecting atmospheric element deposition (Brunialti and Frati, 2014; Vannini et al., 2017; Zhao et al., 2019; Jia et al., 2020). Typically, the effective exposure time span for lichens is between 1 to 4 months, during which element concentrations reach equilibrium between lichen transplants and the atmosphere (Bačkor and Loppi, 2009; Aprile et al.,

2010; Kularatne and de Freitas, 2013; Brunialti and Frati, 2014; Gao et al., 2022). The size of the effective exposure time span, retention time and equilibrium time tends to be element- and species-specific, and is also influenced by air pollution level and other environmental factors (Godinho et al., 2008; Bačkor and Loppi, 2009; Paoli et al., 2018; Zhao et al., 2019; Jia et al., 2020).

Secondly, understanding how the bioaccumulation rate of *RSI* varies with exposure time remains undetermined. This lack of knowledge limits our ability to accurately interpret biomonitoring results when using interpretive scales for lichen transplants. As described in previous studies (Reis et al., 1999; Bačkor and Loppi, 2009; Godinho et al., 2011), element bioaccumulation in lichen thalli is a dynamic process of passive uptake and loss that ultimately reaches equilibrium with the environment. When exposed to high air pollution, the initially high ratio of lichens' uptake to release gradually decreases until the two rates are approximately equal (Reis et al., 1999). This trend is also evident in a five-class interpretive scale for lichen transplants (*Table S1*) proposed by Cecconi et al. (2019). In this scale, the EU thresholds between classes do not increase linearly with exposure time (*Fig. 1a*), indicating a non-linear relationship between bioaccumulation and time. When calculated as an increment per week $[(EU-1)/\text{exposure weeks} \times 100\%]$, the bioaccumulation rate clearly decreases with longer exposure times (*Fig. 1b*). In conclusion, while theoretical understanding and some scale-based indications suggest a decrease in the bioaccumulation rate of lichen with exposure time, more direct empirical evidence is urgently needed to firmly establish this relationship and enhance the accuracy of biomonitoring interpretations using *RSI*.

We transplanted *RSI* samples (*Fig. 2c*) from a remote “clean” site (Saihanba; *Fig. 2a*) to 22 sites of a typical industrial city in China (Tangshan; *Fig. 2b*). The exposures regimen included two 2-month exposure time spans (Nov. 2016-Jan. 2017, NJ2; and Jan.-Mar. 2017, JM2) and one 4-month exposure time span (Nov. 2016-Mar. 2017, NM4; *Fig. 2d*). Concentrations of 47 elements were analyzed. The hypotheses of this study are as follows: 1) The effective exposure time span for *RSI* is 2-4 months, during which the spatial and temporal patterns of *RSI* element bioaccumulation are both qualitatively and quantitatively similar to those of atmospheric suspended particulate matters (PMs). 2) The bioaccumulation rate may decrease during the late stage of a 4-month exposure, suggested by the higher sum bioaccumulation in the NJ2 and JM2 exposures compared to the NM4 exposure. Our research is novel in that it represents one of the few quantitative studies into two key aspects. First, it examines the relationship between *RSI* element and atmospheric suspended PM concentrations, assessing the accuracy of *RSI* bioaccumulation in mirroring atmospheric PM levels. Second, it determines *RSI*'s effective exposure time and assesses its sensitivity in reflecting atmospheric element deposition.

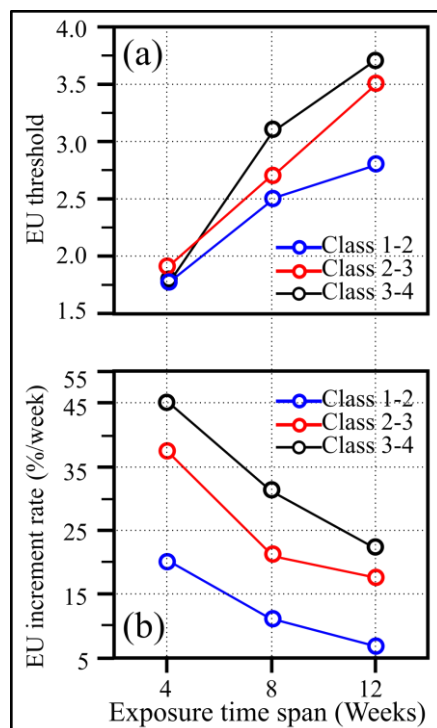


Figure 1. (a) EU thresholds between classes in a five-class interpretive scale for lichen transplants. (b) EU increment rate in different exposure time spans derived from a five-class interpretive scale for lichen transplants. EU ratio denotes exposed to unexposed ratio. The five-class interpretive scale for lichen transplants is from Cecconi et al. (2019) and detailed in Table S1. EU increment rate is calculated by $(EU-1)/\text{exposure weeks} \times 100\%$

Materials and methods

Background area, sampling and sample preparation

The background area is Saihanba Forest Farm, located in Hebei Province, North China (Fig. 2a). It has been used as a background area in active lichen biomonitoring studies (Li et al., 2024; Lin et al., 2024). The climate is a typical cold temperate continental monsoon climate, with an annual average precipitation of 438 mm. The average annual temperature is $-1.2\text{ }^{\circ}\text{C}$, with an extreme minimum temperature of $-43.3\text{ }^{\circ}\text{C}$ and an extreme maximum temperature of $33.4\text{ }^{\circ}\text{C}$. The ecosystem is a montane forest ecosystem, with altitudes ranging from 1100 to 1940 m and a forest coverage of up to 80%. The predominant vegetation consists of *Larix gmelinii* (Rupr.) Kuzen. and *Betula platyphylla* Suk, which support abundant thalli of *RSI* on their bark. The area is sparsely populated, situated approximately 50 km from the densely populated downtown area of Weichang County. The air quality is excellent, exhibiting low concentrations of atmospheric suspended particulates ($\text{PM}_{2.5}$ and PM_{10} ; Fig. 2e-f).

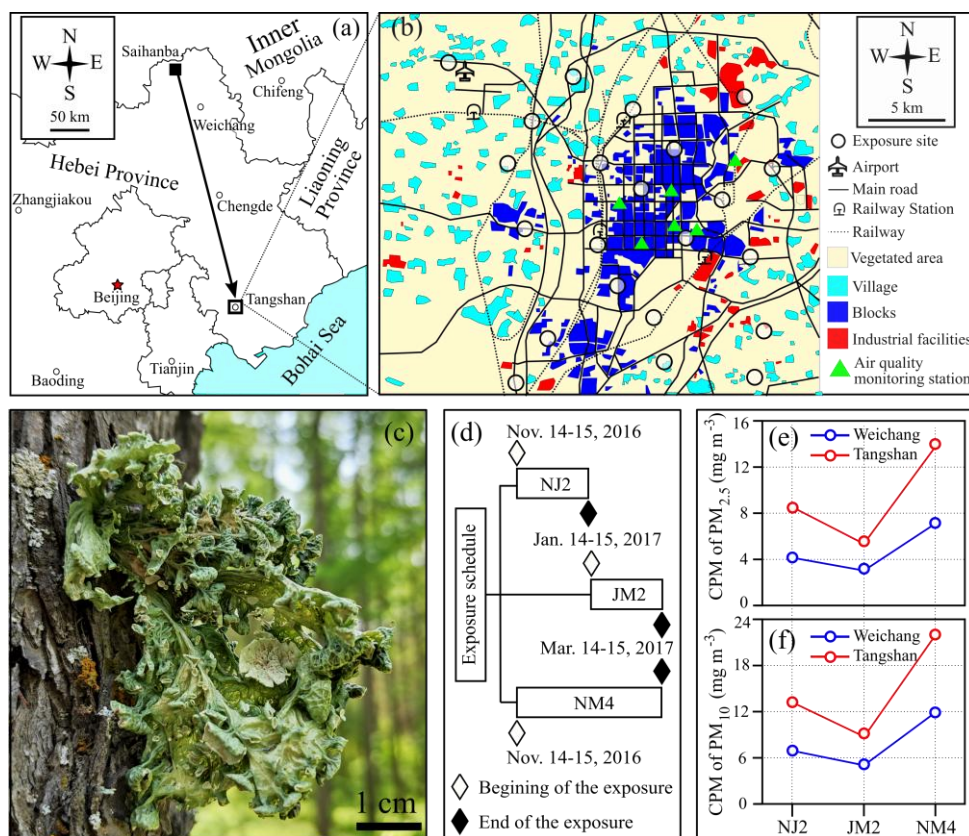


Figure 2. (a) Location of background and exposure areas. (b) Habitat and exposure sites in Tangshan. (c) *Ramalina sinensis* in the background area. (d) Schedule of three exposures. (e) CPM of PM_{2.5} in background and exposure sites in the three exposure periods. (h) CPM of PM₁₀ in background and exposure sites in the three exposure periods. CPM denotes cumulative daily mean concentration of atmospheric suspended particulate matters and was calculated by (Eq.1)

RSI serves as a good bioaccumulator for atmospheric metal depositions in urban areas of North China and Iran (Tumur et al., 2011; Sohrabi et al., 2021; Li et al., 2024). It is a corticolous foliose lichen, distinguished by its large dorsoventral thallus, large lobes (5-10 mm in width) and irregular ridges on the upper surface (Fig. 2c). On Oct. 23, 2016, we collected *RSI* samples along a line transect (42°26'7"N, 117°9'29"E) measuring 50 × 1000 m at an altitude of 1500 m. To minimize the potential effects of collection height and aspect on lichen element concentrations (Adams and Gottardo, 2012), we randomly collected samples by hand from various aspects of the bark of *Larix gmelinii* and *Betula platyphylla* trees, at a height of 1 to 2 m above the ground, as has been adopted in many relevant studies (Agnan et al., 2014; Klos et al., 2018; Dörter et al., 2020).

In the laboratory, we carefully cleaned the lichen thalli to remove any impurities under a stereomicroscope (Motic SMZ-140). *RSI* thalli were rinsed with deionized water 3 to 5 times, with each rinse lasting 5 seconds, in order to reduce element concentrations and their variability (Godinho et al., 2009b). A total of 203 samples were used in this study,

comprising 5 unexposed and 198 exposed samples (22 exposure sites \times 3 replicates \times 3 exposures). Each sample was a composite consisting of 10 to 15 thalli, each thallus measuring 2 to 4 cm in length, to enhance the representativeness of the samples (Zheng et al., 2023). The unexposed samples were stored in sealed kraft bags at room temperature, while the exposed samples were placed in nylon bags measuring 10 \times 15 cm.

Exposure area and lichen exposure

The exposure area is Tangshan city, Hebei Province, North China (Fig. 2a,b). The climate is a warm temperate semi-humid continental monsoon climate, with annual precipitation of 500 to 700 mm. The average annual temperature is 12.5 °C, with an extreme minimum temperature of -20.0 °C and an extreme maximum temperature of 38.0 °C. Tangshan is a typical industrial city with severe air pollution in North China, particularly during winter heating period. In 2015, Tangshan represented 6.6% of the land area and 7.0% of the population within the Beijing-Tianjin-Hebei region, however, it was responsible for 45% of the steel enterprises and approximately 40% of atmospheric PM emissions from the steel industries in the region (Duan et al., 2018). During the exposure period, data from six meteorological monitoring stations (Fig. 2b) show that the cumulative daily mean concentration of atmospheric suspended PMs (CPM) in the exposure area was significantly higher than that in the background area (Fig. 2e-f). According to a five-class interpretive scale (Table S1; Cecconi et al., 2019) and previously published data, the element bioaccumulation level in *RSI* transplants in the exposure area were classified as class 3 (moderate bioaccumulation), with element-specific cross-site variability ranging from class 2 to 5 (low to severe bioaccumulation) (Li et al., 2024).

Twenty-two exposure sites with similar altitude (20-50 m) were carefully selected to represent a variety of environments, including industrial facilities, residential sites, agricultural lands, railway stations, and airports (Fig. 2b). The shortest distance between these sites is 2-5 km. GPS position and environment of these sites are detailed in Lin et al. (2024). Three exposures were performed at each site (Fig. 2d), comprising two 2-month exposure time spans (Nov. 2016 to Jan. 2017, NJ2; and Jan. to Mar. 2017, JM2) and one 4-month exposure time span (Nov. 2016 to Mar. 2017, NM4). Each site included 3 replicates. The nylon bags containing samples were hung to the trunks of *Populus* spp. at a height of 2.5 m.

Sample recovery and element determination

Exposure samples were recovered at the end of the three exposures (Fig. 2d). The samples were carefully cleaned to remove surface impurities using tweezers and a soft brush under a stereomicroscope, oven-dried for 72 h at 72 °C to constant weight, and subsequently ground and homogenized using a ball grinder (Retsch MM400; Retsch GmbH, Haan, Germany). An aliquot of 200-300 mg of the samples were then mineralized in a mixture of HNO₃-H₂O₂ using microwave digestion. The resulting digested solution was sealed and stored for further analysis.

Element concentrations, expressed in $\mu\text{g}\cdot\text{g}^{-1}$ dry weight, were tested using inductively coupled plasma mass spectrometry (ICP-MS, Agilent 7700X, Agilent Technologies, Tokyo, Japan). Concentrations for 47 elements were used in this study. These elements are Al, B, Ba, Be, Bi, Ca, Cd, Cr, Cs, Cu, Fe, Ge, K, Li, Mg, Mn, Mo, Na, Nb, Ni, Pb, Rb, Sb, Se, Si, Sn, Sr, Ti, Tl, V, and Zn, as well as 16 REEs (Sc, La, Ce, Pr, Nd, Sm, Eu, Gd, Tb, Dy, Ho, Er, Tm, Yb, Lu, and Y). For quality control purpose, three reference materials from the Institute of Geophysical and Geochemical Exploration, Chinese Academy of Geological Sciences were used: GBW10014 (cabbage), GBW10015 (spinach) and GBW10052 (green tea).

Concentration of atmospheric suspended PMs

The cumulative daily mean concentration of atmospheric suspended particulate matter (CPM) during the three exposure periods was calculated by *Eq.1*:

$$\text{CPM} = \sum_{i=1}^n C_i \quad (\text{Eq.1})$$

where C_i is the daily mean concentration of the i -th day of exposure, n is the total number of days exposed.

The average daily mean concentration of atmospheric suspended particulate matter (APM) was calculated as the ratio of CPM to the number of exposure days. The daily mean concentration of PMs was obtained from two meteorological stations in Weichang County for the background area, and from six meteorological stations in Tangshan City for the exposure area (*Fig. 2b*).

EU ratio and PLI

EU ratio was calculated using *Eq.2*:

$$\text{EU} = C_{\text{exposed}} / C_{\text{unexposed}} \times 100\% \quad (\text{Eq.2})$$

where “C” represents the concentration, “exposed” represents the exposed sample, “unexposed” represents the unexposed sample.

EU_{NJ2} , EU_{JM2} and EU_{NM4} represent EU ratios for NJ2, JM2 and NM4 exposures, respectively. The expected EU_{NM4} was calculated using *Eq.3*:

$$\text{Expected } \text{EU}_{\text{NM4}} = (\text{EU}_{\text{NJ2}} + \text{EU}_{\text{JM2}}) - 1 \quad (\text{Eq.3})$$

Pollution load index at site scale (PLI_{site}) was calculated using *Eq.4*:

$$\text{PLI}_{\text{site}} = (\text{EU}_{\Sigma\text{REE}} \times \text{EU}_2 \times \dots \times \text{EU}_n)^{1/n} \quad (\text{Eq.4})$$

where “ Σ REE” represents a geometric mean of EU ratios of 16 REEs (14 lanthanoids, and Sc and Y), “n” represents number of elements. REEs are considered as one element because their EU ratios are very similar.

Pollution load index at regional scale (PLI_{zone}) was calculated using Eq.5:

$$PLI_{zone} = (PLI_{site-1} \times PLI_{site-2} \times \dots \times PLI_{site-n})^{1/n} \quad (Eq.5)$$

where “ PLI_{site-n} ” represents the PLI_{site} at the n-th site.

Statistical analysis

Data normality was assessed using Shapiro-Wilk test. For datasets following a normal/log-normal distribution, the coefficient of variation (CV) was used to assess variability, otherwise the robust coefficient of variance (CV') was used. CV and CV' were calculated using Eq.6 and Eq.7, respectively:

$$CV = SD/mean \times 100\% \quad (Eq.6)$$

where mean represents average of the data, SD represents standard deviation.

$$CV' = (Q3 - Q1) \times 0.7413 / Med. \times 100\% \quad (Eq.7)$$

where Q1 represents upper quartile, Q3 represents lower quartile, Med. represents median.

When testing the differences between unexposed and exposed concentrations, an independent samples T test was used for data following normal/log-normal distribution, otherwise a Mann-Whitney U test was used. When testing the differences of EU and PLI_{site} across three exposures, independent groups tests were preferred over paired samples tests to minimize the effects of spatial pattern differences in air pollutants between the NJ2 and JM2 exposures. A one-way analysis of variance (ANOVA) with Tukey's Honestly Significant Difference (HSD) post-hoc analysis was applied to data following normal/log-normal distribution, otherwise the Mann-Whitney U test with Bonferroni correction for multiple comparisons following the Kruskal-Wallis H test was used. When testing the differences between observed and expected EU_{NM4} , a paired samples T test was conducted for data following a normal/log-normal distribution, otherwise Wilcoxon rank sum test was used. The significance level for all statistical tests was set at $\alpha = 0.05$. All analyses were conducted using SPSS 21.0 (SPSS Inc., Chicago, IL, USA).

Results

Element concentrations in RSI

Table 1 presents the unexposed concentrations in RSI. The unexposed concentrations were of normal distribution for all elements (Shapiro-Wilk test, $\alpha = 0.05$), and had CV and CV' of < 22% for all elements except Al (CV = 22.48%; CV' = 27.96%).

Table 1. Unexposed concentration and variability (CV and CV') for 47 elements in *Ramalina sinensis*

Unexposed concentration (n = 5)									
	Mean ($\mu\text{g}\cdot\text{g}^{-1}$)	CV (%)	CV' (%)	Norm.		Mean ($\mu\text{g}\cdot\text{g}^{-1}$)	CV (%)	CV' (%)	Norm.
Al	1180	22.48	27.96	N	Si	3657	15.74	21.71	N
B	2.181	6.20	8.56	N	Sn	0.233	5.78	6.58	N
Ba	9.178	5.63	7.42	N	Sr	4.474	5.29	7.03	N
Be	0.034	5.36	7.67	N	Ti	57.71	6.27	7.96	N
Bi	0.089	5.76	8.04	N	Tl	0.033	4.96	6.47	N
Ca	1050	10.79	14.37	N	V	1.800	5.05	6.84	N
Cd	0.135	6.05	7.95	N	Zn	21.62	2.69	3.75	N
Cr	2.153	7.94	10.61	N	Rare earth elements				
Cs	0.191	5.26	6.48	N	Sc	0.281	4.32	5.84	N
Cu	4.138	3.71	4.47	N	Y	0.561	4.06	5.68	N
Fe	692.5	4.82	6.21	N	La	0.940	3.68	4.96	N
Ge	0.137	4.91	7.06	N	Ce	1.803	3.68	4.82	N
K	2752	4.98	6.27	N	Pr	0.207	4.19	5.51	N
Li	0.625	4.73	6.26	N	Nd	0.807	4.34	5.84	N
Mg	406.7	4.01	5.51	N	Sm	0.153	4.08	5.27	N
Mn	24.11	5.48	6.21	N	Eu	0.032	4.65	6.55	N
Mo	0.143	6.59	8.43	N	Gd	0.134	4.19	5.57	N
Na	153.9	5.90	7.97	N	Tb	0.019	5.39	7.33	N
Nb	0.097	5.60	7.40	N	Dy	0.105	4.46	6.36	N
Ni	0.978	4.02	5.36	N	Ho	0.020	3.80	5.49	N
Pb	2.393	2.62	3.41	N	Er	0.055	4.31	6.38	N
Rb	3.731	5.74	7.54	N	Tm	0.008	4.33	5.92	N
Sb	0.086	5.10	5.95	N	Yb	0.049	4.04	5.77	N
Se	0.308	4.33	5.81	N	Lu	0.007	4.82	6.93	N

In Norm. column, "N" indicates normal distribution. CV and CV' were calculated using (Eq.6) and (Eq.7), respectively

Table 2 summarizes the exposed concentrations; for further details, please refer to supplementary Tables S2-S4. At the regional scale, exposed concentrations were higher than unexposed concentrations for all elements across the three exposures, except Bi and Cd in the JM2 exposure (Independent samples T test or Mann-Whitney U test, $p \leq 0.05$; Table 2). Over 89% of the elements in the NJ2 (43 elements) and JM2 (42) exposures exhibited a normal/log-normal distribution, in contrast to only 32% of the elements in the NM4 exposure (15). We used CV' to assess global variability of exposed concentrations due to the data normality of NM4 exposure. The exposed concentrations had a greater global variability (CV') than the unexposed concentrations for all elements but Al and Si.

Table 2. Exposed concentrations of 47 elements in *Ramalina sinensis* in the three exposures

	NJ2 (n = 22)				JM2 (n = 22)				NM4 (n = 22)			
	Norm.	Mean ($\mu\text{g}\cdot\text{g}^{-1}$)	CV (%)	CV' (%)	Norm.	Mean ($\mu\text{g}\cdot\text{g}^{-1}$)	CV (%)	CV' (%)	Norm.	Mean ($\mu\text{g}\cdot\text{g}^{-1}$)	CV (%)	CV' (%)
Al	N	2675*	25.84	33.54!	N	1881*	17.11	20.08	N	2287*	25.68	22.84
B	Non	10.22*	32.27	34.95!	N	10.66*	16.70	20.00!	Non	13.97*	28.13	16.34!
Ba	N	24.36*	19.90	22.79!	Non	17.23*	29.15	21.20!	Non	25.69*	28.91	21.28!
Be	N	0.072*	21.48	21.78!	N	0.053*	14.30	14.50!	Non	0.072*	24.20	21.37!
Bi	N	0.109*	18.90	17.81!	N	0.108	25.13	27.85!	N	0.127*	22.41	16.28!
Ca	LN	3973*	30.81	33.19!	Non	1618*	44.00	37.86!	Non	3812*	29.75	22.74!
Cd	Non	0.305*	31.62	23.58!	Non	0.145	19.13	17.65!	LN	0.298*	41.69	35.45!
Cr	N	5.283*	19.23	21.63!	N	3.737*	18.65	16.60!	Non	5.398*	24.81	21.18!
Cs	N	0.323*	19.22	20.85!	N	0.256*	14.17	17.97!	Non	0.342*	21.95	19.28!
Cu	N	6.880*	16.44	21.97!	Non	5.610*	17.10	15.96!	LN	6.756*	20.26	15.79!
Fe	N	1808*	23.29	21.38!	N	1213*	15.35	14.95!	LN	1841*	22.59	24.97!
Ge	N	0.210*	19.22	18.49!	N	0.160*	12.36	12.59!	Non	0.218*	23.04	20.32!
K	N	4136*	15.11	12.08!	LN	3706*	15.59	13.65!	N	3822*	13.19	17.23!
Li	LN	1.535*	24.72	21.23!	N	1.075*	15.12	17.30!	N	1.715*	22.85	21.46!
Mg	N	1178*	24.17	22.58!	N	702.5*	13.93	15.14!	Non	1181*	28.42	20.99!
Mn	N	71.51*	27.23	26.73!	N	42.54*	14.20	13.07!	Non	70.73*	29.76	26.11!
Mo	N	0.265*	21.44	24.96!	N	0.184*	16.53	19.22!	Non	0.271*	27.60	21.82!
Na	LN	808.1*	42.29	43.65!	N	342.8*	19.73	16.61!	Non	867.5*	53.40	36.61!
Nb	N	0.171*	20.04	17.33!	N	0.146*	14.54	15.08!	LN	0.187*	20.73	18.86!
Ni	N	2.321*	20.42	17.90!	N	1.630*	18.33	19.28!	Non	2.369*	25.53	21.16!
Pb	N	6.064*	21.88	21.18!	N	3.575*	16.07	17.95!	N	6.391*	18.46	15.25!
Rb	Non	5.962*	26.65	13.97!	N	4.661*	14.09	12.89!	N	5.685*	19.79	23.03!
Sb	N	0.239*	22.30	25.83!	N	0.123*	17.92	20.59!	N	0.234*	25.68	28.80!
Se	N	0.535*	15.36	17.65!	N	0.383*	12.48	14.14!	Non	0.519*	20.11	18.09!
Si	N	6963*	21.02	24.45!	N	5200*	16.35	18.03	N	7113*	27.34	22.55!
Sn	N	0.346*	16.96	16.34!	N	0.294*	18.62	22.44!	N	0.358*	13.97	14.77!
Sr	N	12.72*	22.01	22.74!	N	7.021*	21.07	24.85!	Non	12.95*	24.31	16.89!
Ti	N	101.5*	18.79	18.19!	N	82.95*	14.31	18.71!	Non	104.2*	21.25	19.08!
Tl	N	0.085*	21.97	22.56!	N	0.053*	14.29	14.57!	N	0.093*	24.75	24.78!

	NJ2 (n = 22)				JM2 (n = 22)				NM4 (n = 22)			
	Norm.	Mean ($\mu\text{g}\cdot\text{g}^{-1}$)	CV (%)	CV' (%)	Norm.	Mean ($\mu\text{g}\cdot\text{g}^{-1}$)	CV (%)	CV' (%)	Norm.	Mean ($\mu\text{g}\cdot\text{g}^{-1}$)	CV (%)	CV' (%)
V	N	3.932*	22.47	22.40!	N	2.733*	13.60	13.25!	Non	3.908*	25.32	22.42!
Zn	Non	76.28*	39.18	37.89!	Non	30.61*	24.05	21.96!	Non	68.31*	41.77	36.83!
Rare earth elements												
Sc	N	0.484*	20.17	17.54!	N	0.413*	15.43	14.64!	Non	0.499*	21.27	21.64!
Y	N	0.942*	18.67	18.54!	N	0.770*	14.54	16.15!	Non	0.983*	21.32	23.18!
La	N	1.570*	20.20	22.07!	LN	1.250*	14.81	17.83!	Non	1.647*	21.73	22.34!
Ce	N	3.017*	20.47	22.26!	N	2.445*	14.35	17.55!	Non	3.247*	22.36	23.66!
Pr	N	0.339*	20.52	22.03!	N	0.281*	14.12	16.15!	LN	0.367*	22.15	22.03!
Nd	N	1.316*	20.22	22.03!	N	1.089*	13.57	15.62!	Non	1.423*	22.48	21.20!
Sm	N	0.249*	19.90	21.78!	N	0.204*	14.26	15.36!	Non	0.259*	23.62	25.35!
Eu	N	0.055*	19.95	21.18!	N	0.044*	13.61	15.44!	Non	0.056*	22.67	21.48!
Gd	N	0.217*	20.09	21.19!	N	0.181*	14.63	14.51!	Non	0.225*	23.09	21.34!
Tb	N	0.030*	19.56	20.06!	N	0.025*	14.69	15.98!	Non	0.032*	22.49	23.53!
Dy	N	0.172*	19.07	19.74!	N	0.144*	14.83	16.70!	Non	0.181*	22.77	22.84!
Ho	N	0.033*	18.81	18.83!	N	0.027*	14.14	18.22!	Non	0.034*	22.72	22.63!
Er	N	0.091*	18.85	19.50!	N	0.075*	13.77	16.55!	Non	0.096*	22.27	20.63!
Tm	N	0.013*	18.70	22.12!	N	0.011*	13.78	16.33!	Non	0.013*	23.52	21.51!
Yb	N	0.081*	18.55	18.50!	N	0.067*	13.43	17.28!	Non	0.084*	22.38	22.82!
Lu	N	0.012*	19.14	21.87!	N	0.012*	13.12	15.70!	Non	0.012*	23.27	23.74!

In Norm. column, “N” indicates normal distribution; “Non” indicates no normal distribution. “LN” indicates log-normal distribution. In Mean column, “*” indicates that the exposed concentration was significantly higher than the unexposed concentration, otherwise no significant difference was found between the exposed and unexposed concentrations. In CV' (%) column, “!” indicates that CV' was higher in the exposed concentrations than in the unexposed ones. For elements with exposed concentrations following normal distribution, an independent samples T test were conducted to test the difference between the exposed and unexposed concentrations, otherwise a Mann-Whitney U test were conducted. CV and CV' were calculated using (Eq.6) and (Eq.7), respectively. Part of the NM4 data has been published in Li et al. (2024). At the site scale, 87.6% of the data points for the exposed concentrations (2,717 out of 3,102) were higher than the unexposed concentrations, while the remaining data points were similar to the unexposed concentrations (Fig. S1; independent samples t-test, $\alpha = 0.05$).

At the site scale, 87.6% of the data points for the exposed concentrations (2,717 out of 3,102) were higher than the unexposed concentrations, while the remaining data points were similar to the unexposed concentrations (*Fig. S1*; independent samples t-test, $\alpha = 0.05$).

EU ratio and PLI

Fig. 3(a) illustrates the EU ratios and PLI_{site} across the three exposures. Both the EU ratios and PLI_{site} were higher in the NM4 exposure than in the JM2 exposure for all elements. EU ratios for B, Bi, and K were higher in the NM4 exposure than in the NJ2 exposure, and were similar between the NJ2 and JM2 exposures. For the remaining 44 elements, the EU ratios and PLI_{site} were similar between the NM4 and NJ2 exposures, and were higher in the NJ2 exposure than in the JM2 exposure (One-way ANOVA with a Tukey's HSD test for multiple comparisons, or a Mann-Whitney U test following a Kruskal-Wallis test with a Bonferroni correction for multiple comparisons; $\alpha = 0.05$; *Table S5*). The PLI_{zone} values for the NJ2, JM2, and NM4 exposures were 2.20, 1.51, and 2.24, respectively.

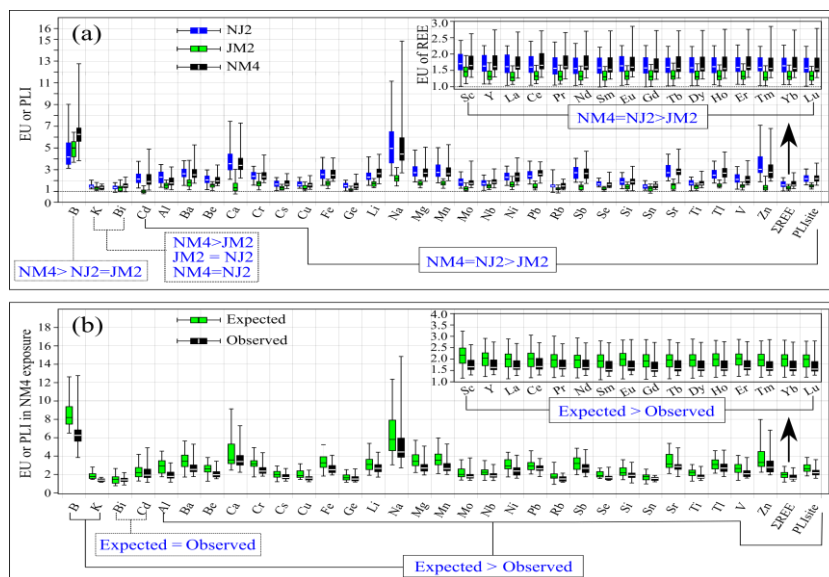


Figure 3. (a) Boxplot of EU and PLI_{site} for elements in *Ramalina sinensis* in three exposures. Differences between exposures were noted in the figure. Differences were tested by One-way ANOVA with Tukey's HSD test for multicomparisons or by Mann-Whitney U test after Kruskal-Wallis test with Bonferroni correction for multicomparisons, depending on data normality. The ANOVA and Kruskal-Wallis test results were presented in *Table S5*. NJ2 denotes exposure time of Nov. 2016 to Jan. 2017. JM2 denotes exposure time of Jan. to Mar. 2017. NM4 denotes exposure time of Nov. 2016 to Mar. 2017. (b) Boxplot of EU and PLI_{site} for elements in *Ramalina sinensis* in NM4 exposure. Differences between the observed and expected values were noted in the figure. Differences were tested by Paired-samples T test or Wilcoxon rank sum test, depending on data normality. Elements were arranged first according to difference then alphabetically. $n = 22$ for each box

Fig. 3(b) illustrates the expected and observed EU ratios and PLI_{site} in the NM4 exposure. The expected EU_{NM4} was higher than the observed EU_{NM4} for all elements except for Bi and Cd, for which the expected EU_{NM4} was similar to the observed values (Paired-samples T test or Wilcoxon rank sum test, $\alpha = 0.05$).

Table 3 shows the ratios between exposures for the PLI_{zone} and PM parameters. The NJ2:JM2 ratio was similar between the PLI_{zone} and PM parameters. However, both NM4:NJ2 and NM4:JM2 ratios were dissimilar between PLI_{zone} and PM parameters.

Table 3. Ratios between exposures for the PLI_{zone} and parameters of atmospheric particulate matters

Ratio between exposures	PM parameters				PLI_{zone} of <i>Ramalina sinensis</i>
	APM		CPM		
	PM_{10}	$PM_{2.5}$	PM_{10}	$PM_{2.5}$	
NJ2:JM2	1.44	1.49	1.51	1.56	1.46
NM4:NJ2	0.85	0.84	1.66	1.64	1.02
NM4:JM2	1.22	1.25	2.51	2.56	1.48

PM denotes the atmospheric particulate matters. APM denotes the average daily mean concentration of atmospheric particulate matters. CPM denotes the cumulative daily mean concentration of atmospheric particulate matters (CPM). NJ2 denotes the exposure time of Nov. 2016 to Jan. 2017. JM2 denotes the exposure time of Jan. to Mar. 2017. NM4 denotes the exposure time of Nov. 2016 to Mar. 2017

Discussion

Unexposed and exposed concentrations: setting stage for hypotheses testing

We adopted rigorous protocols for active lichen biomonitoring to test the two hypotheses, as they produce higher quality data than the less-rigorous protocols (Will-Wolf et al., 2017). As a result, we got the lower, less variable unexposed concentrations and the higher exposed concentrations, which helps to minimize type-II errors or false negatives in comparing the unexposed and exposed concentrations.

Our protocols provide homogeneous unexposed concentrations for all elements. The low variability ($CV < 23\%$; $CV' = 28\%$; Table 1) is consistent with relevant studies, which suggest a background or local variability of $\leq 30\%$ (Ayrault et al., 2007; Godinho et al., 2009a; Wu et al., 2020). Lichen element concentrations can be strongly affected by micro-environmental conditions and atmospheric contaminant dispersions (Adams and Gottardo, 2012). However, these effects can be minimized by using rigorous sampling protocols in the background area, such as random sampling at a constant height (1-2 m from the ground) and from all aspect of tree barks, within a small sampling size (50×1000 m) at a constant altitude (1500 m). We also controlled the thalli size (2-4 cm long), as young thalli often have lower concentrations for non-nutrient elements and a higher accumulation capability for heavy metals than the older thalli (Godinho et al., 2009a). Washing the samples with deionized water before exposure can lower both concentrations

and variability of the unexposed samples (Godinho et al., 2009b; Demiray et al., 2012). Additionally, using a composite sample consisting of 10-15 thalli can increase sample representativeness by reducing local variability in lichen element concentrations (Zheng et al., 2023).

Our protocols provide a higher and more variable air pollution in the exposure area compared to the background area (*Fig. 2e-f*). By selecting Tangshan, a typical industrially polluted city, we got higher exposed concentrations compared to the unexposed ones for most elements at regional (*Table 2*) and local scales (*Fig. S1*). Additionally, by selecting 22 sites that covering various environments, we achieved higher global variability in the exposed concentrations than in the unexposed ones for most elements (CV' ; *Table 2*). This is further supported by published data of NM4 exposure (Li et al., 2024). According to a five-class interpretive scale for lichen transplants (*Table S1*) (Cecconi et al., 2019), bioaccumulation level in NM4 exposure belongs to class 3 (moderate bioaccumulation) with a high variability ranging from class 2 to 5 (light to severe bioaccumulation) for most elements (Li et al., 2024).

Effective exposure time span for RSI

Our findings confirm hypothesis 1: *RSI* effective exposure time span is 2-4 months. Element concentrations in *RSI* mirrored atmospheric pollutant levels in our study, which is a theoretical basis for lichen biomonitoring methods (Garty, 2001). The exposed area showed higher element concentrations than the background area at the local (*Fig. S1*) and regional scales (*Table 2*), matching higher CPM levels (*Fig. 2e-f*). Both NM4 and NJ2 exposures yielded higher EU ratios and PLI_{site} values than the JM2 exposure for most elements (*Fig. 3a*), aligning with CPM temporal patterns (*Fig. 2e-f*). Active biomonitoring studies in urban sites of Iran and China qualitatively corroborate our findings, revealing elevated concentrations in *RSI* transplants at polluted sites compared to cleaner areas (Tumur et al., 2011; Sohrabi et al., 2021; Gao et al., 2022; Li et al., 2024). This spatial and temporal consistency underscores *RSI*'s reliability as a biomonitoring tool for atmospheric contaminants.

Different from previous studies, we present quantitative evidence of spatial and temporal alignment between *RSI* element levels and air pollution. The 2-month exposures revealed proportional bioaccumulation in *RSI* to airborne suspended particulate concentrations, evidenced by comparable NJ2:JM2 ratios for PLI_{zone} and PM parameters (*Table 3*). This confirms the effective exposure time span of two months for *RSI*. Although quantitative evidence for 4-month exposure time spans is lacking due to limited data, the observed element-contaminant consistency suggests this longer duration is also effective. These findings support the notion that a 4-month exposure time span is also effective for *RSI*.

Bioaccumulation rate changes with exposure time

Our findings confirm hypothesis 2: *RSI* bioaccumulation decreases in the late stage of 4-month exposure. The NM4 and NJ2 exposures show similar EU ratios for 46/47 elements (Fig. 3a). In NM4 exposure, the observed bioaccumulation is significantly lower than the expected one for 45/47 elements (Fig. 3b). These results indicate *RSI* primarily accumulates elements in the first 2 months, with nearly 0 uptake thereafter.

The bioaccumulation predominance in the first 2 months suggests a retention time < 2 months for *RSI*, with minimal time-lag effects on *RSI* bioaccumulation. This is particularly supported by NM4 exposure, where the expected bioaccumulation (containing two retention time periods) exceeds the observed bioaccumulation (containing one retention time period; Fig. 3b). This retention time is rather short compared to the relevant studies. *Evernia prunastri* transplants near cement mill and quarries showed a retention time of < 30 days for the dust-associated elements (Paoli et al., 2016). *Flavoparmelia caperata* transplants in an industrial zone showed a retention time of ≥ 2 months for most metals (Godinho et al., 2008). Three lichens (*Xanthoparmelia camtschadalis*, *Flavopunctelia soledica*, and *Rhizoplaca chrysoleuca*) transplanted to busy roads exhibited retention times of <3 months for S and > 3 months for metals (Zhao et al., 2019; Jia et al., 2020).

The 0 bioaccumulation in the latter 2-months points to an equilibrium time of 2 months for *RSI*, within ranges of other studies. Most of the active lichen biomonitoring studies report positive bioaccumulation in 3-month exposures, but 0 or negative bioaccumulation in longer exposures, depending on species of elements and lichens, level of atmospheric deposition and environmental climate conditions (Godinho et al., 2011; Gallo et al., 2017; Lucadamo et al., 2018; Loppi et al., 2019). Equilibrium times range widely across lichen species and pollution conditions. For example, the equilibrium is 30 days for *Evernia prunastri* in a less-polluted area (Loppi and Paoli, 2015), 7 months for *RSI* in a heavy polluted city (Gao et al., 2022), 9 months for *Flavopunctelia soledica*, *Rhizoplaca chrysoleuca* and *Xanthoparmelia camtschadalis* near busy roads (Zhao et al., 2019; Jia et al., 2020), and 12-15 months for *Parmotrema reticulatum* in industrial areas (Kularatne and de Freitas, 2013).

The 0 bioaccumulation in the latter 2 months may stem from the intensified effects of various factors on *RSI* transplants with extended exposure time. The NM4 exposure showed more elements with non-normal distribution (accounting for 68% of the total elements) compared to the shorter exposures (NJ2, 8.5%; JM2, 10.6%; Table 2). This reduced normality indicates increasing effects of factors other than atmospheric deposition on *RSI* bioaccumulation over time. Within the effective exposure time spans, bioaccumulation is less affected by retention and equilibrium time (Godinho et al., 2011; Gallo et al., 2017; Lucadamo et al., 2018; Loppi et al., 2019), but is more affected by the lichen biological properties (Malaspina et al., 2014; Cecconi et al., 2021). These properties interact strongly with lichen bioaccumulation, both strongly affected by

atmospheric pollution, climate and landscape variability (Vannini et al., 2017; Cecconi et al., 2021; Bajpai et al., 2022; Kováčik et al., 2023; Kumari et al., 2024). The stark contrast between the remote background montane forest and industrial polluted plain city (Duan et al., 2018; Li et al., 2024; Lin et al., 2024) likely drives the site-dependent biological and further bioaccumulation variability in *RSI* transplants in Tangshan.

Conclusion

RSI serves as a good active biomonitor, accurately and sensitively mirroring the availability of atmospheric suspended PMs through its element composition. PLI_{zone} and PM parameters showed similar NJ2:JM2 ratios, suggesting a high accuracy of *RSI* bioaccumulation reflecting atmospheric suspended PM availability in 2-month exposures. Bioaccumulation primarily occurs within the first two months of the 4-month exposure, suggesting a retention time of < 2 months and an equilibrium time of approximately 2 months, and therefore a high sensitivity of *RSI* bioaccumulation reflecting atmospheric suspended PM availability. The data normality of element concentrations in *RSI* transplants decreased markedly during the 4-month exposure compared to the 2-month exposures, suggesting that the effects of various factors on lichen bioaccumulation intensify with longer exposure time.

In summary, while the effective exposure time span is 2-4 months for *RSI*, it is crucial to note the significant reduction in bioaccumulation rates due to intensified effects of various factors on lichen bioaccumulation performance after the initial 2-month exposure.

Acknowledgments. The authors would like to thank the funding support from Natural Science Foundation of Hebei Province (D2020201002).

REFERENCES

- [1] Abas, A. (2021): A systematic review on biomonitoring using lichen as the biological indicator: A decade of practices, progress and challenge. – *Ecological Indicators* 121: 107197.
- [2] Adams, M. D., Gottardo, C. (2012): Measuring lichen specimen characteristics to reduce relative local uncertainties for trace element biomonitoring. – *Atmospheric Pollution Research* 3(3): 325-330.
- [3] Agnan, Y., Séjalondelmas, N., Probst, A. (2014): Origin and distribution of rare earth elements in various lichen and moss species over the last century in France. – *Science of The Total Environment* 487(14): 1-12.
- [4] Aprile, G. G., Di Salvatore, M., Carratù, G., Mingo, A., Carafa, A. M. (2010): Comparison of the suitability of two lichen species and one higher plant for monitoring airborne heavy metals. – *Environmental Monitoring and Assessment* 162(1-4): 291-299.

- [5] Ayrault, S., Clochiatti, R., Carrot, F., Daudin, L., Bennett, J. P. (2007): Factors to consider for trace element deposition biomonitoring surveys with lichen transplants. – *Science of The Total Environment* 372(2): 717-727.
- [6] Bačkor, M., Loppi, S. (2009): Interactions of lichens with heavy metals. – *Biologia Plantarum* 53(2): 214-222.
- [7] Bajpai, R., Shukla, V., Raju, A., Singh, C. P., Upreti, D. K. (2022): A geostatistical approach to compare metal accumulation pattern by lichens in plain and mountainous regions of northern and central India. – *Environmental Earth Sciences* 81(7): 203.
- [8] Boonpeng, C., Polyiam, W., Sriviboon, C., Sangiamdee, D., Watthana, S., Nimis, P., Boonpragob, K. (2017): Airborne trace elements near a petrochemical industrial complex in Thailand assessed by the lichen *Parmotrema tinctorum* (Despr. ex Nyl.) Hale. – *Environmental Science and Pollution Research* 24(13): 12393-12404.
- [9] Boonpeng, C., Sangiamdee, D., Noikrad, S., Boonpragob, K. (2023): Assessing seasonal concentrations of airborne potentially toxic elements in tropical mountain areas in Thailand using the transplanted lichen *Parmotrema Tinctorum* (Despr. ex Nyl.) Hale. – *Forests* 14: 611.
- [10] Brunialti, G., Frati, L. (2014): Bioaccumulation with lichens: The Italian experience. – *International Journal of Environmental Studies* 71(1): 15-26.
- [11] Cecconi, E., Fortuna, L., Benesperi, R., Bianchi, E., Brunialti, G., Contardo, T., Di Nuzzo, L., Frati, L., Monaci, F., Munzi, S., Nascimbene, J., Paoli, L., Ravera, S., Vannini, A., Giordani, P., Loppi, S., Tretiach, M. (2019): New interpretative scales for lichen bioaccumulation data: The Italian proposal. – *Atmosphere* 10(3): 136.
- [12] Cecconi, E., Fortuna, L., Peplis, M., Mauro, T. (2021): Element accumulation performance of living and dead lichens in a large-scale transplant application. – *Environmental Science and Pollution Research* 28: 16214-16226.
- [13] Demiray, A. D., Yolcubal, I., Akyol, N. H., Çobanoğlu, G. (2012): Biomonitoring of airborne metals using the lichen *Xanthoria parietina* in Kocaeli Province, Turkey. – *Ecological Indicators* 18: 632-643.
- [14] Dörter, M., Karadeniz, H., Saklangıç, U., Yenisoy-Karakaş, S. (2020): The use of passive lichen biomonitoring in combination with positive matrix factor analysis and stable isotopic ratios to assess the metal pollution sources in throughfall deposition of Bolu plain, Turkey. – *Ecological Indicators* 113: 106212.
- [15] Duan, W. J., Lang, J. L., Cheng, S. Y., Jia, J., Wang, X. Q. (2018): Air pollutant emission inventory from iron and steel industry in the Beijing-Tianjin-Hebei region and its impact on PM_{2.5}. – *Huan Jing Ke Xue* 39(4): 1445-1454.
- [16] Gallo, L., Corapi, A., Apollaro, C., Vespasiano, G., Lucadamo, L. (2017): Effect of the interaction between transplants of the epiphytic lichen *Pseudevernia furfuracea* L. (Zopf) and rainfall on the variation of element concentrations associated with the water-soluble part of atmospheric depositions. – *Atmospheric Pollution Research* 8(5): 912-920.
- [17] Gao, J., Zhang, L. Y., Li, X., Ma, C. P., Jin, Q., Liu, L., Zhang, J. M., Zhao, L. C., Meng, J. W., Liu, H. J. (2022): Effects of canopy and exposure duration on element composition

- of the transplanted lichen *Ramalina sinensis*. – Chinese Journal of Ecology 41(12): 2289-2298.
- [18] Garty, J. (2001): Biomonitoring atmospheric heavy metals with lichens: Theory and application. – Critical Reviews in Plant Sciences 20(4): 309-371.
- [19] Godinho, R., Wolterbeek, H. T., Verburg, T., Freitas, M. (2008): Bioaccumulation behaviour of transplants of the lichen *Flavoparmelia caperata* in relation to total deposition at a polluted location in Portugal. – Environmental Pollution 151(2): 318-325.
- [20] Godinho, R. M., Verburg, T. G., Freitas, M. C., Wolterbeek, H. T. (2009a): Accumulation of trace elements in the peripheral and central parts of two species of epiphytic lichens transplanted to a polluted site in Portugal. – Environmental Pollution 157(1): 102-109.
- [21] Godinho, R. M., Wolterbeek, H. T., Pinheiro, M. T., Alves, L. C., Verburg, T. G., Freitas, M. C. (2009b): Micro-scale elemental distribution in the thallus of *Flavoparmelia caperata* transplanted to polluted site. – Journal of Radioanalytical and Nuclear Chemistry 281(2): 205-210.
- [22] Godinho, R. M., Verburg, T. G., Freitas, M. C., Wolterbeek, H. T. (2011): Dynamics of element accumulation and release of *Flavoparmelia caperata* during a long-term field transplant experiment. – International Journal of Environment and Health 5: 49-59.
- [23] Jia, S. J., Zhang, X., Liu, Q. X., Chen, Q. Z., Li, X., Pang, X. M., Li, J. J., Wu, Q. F., Zhao, L. C., Liu, H. J. (2020): Spatial-temporal patterns of element concentrations in *Xanthoparmelia camtschadalis* transplanted along roads. – Polish Journal of Environmental Studies 29(1): 121-129.
- [24] Klos, A., Ziembik, Z., Rajfur, M., Dolhanczuk-Srodka, A., Bochenek, Z., Bjerke, J. W., Tommervik, H., Zagajewski, B., Ziolkowski, D., Jerz, D., Zielinska, M., Krems, P., Godyn, P., Marciniak, M., Swislawski, P. (2018): Using moss and lichens in biomonitoring of heavy-metal contamination of forest areas in southern and north-eastern Poland. – Sci Total Environ 627: 438-449.
- [25] Kováčik, J., Husáková, L., Vlassa, M., Piroutková, M., Vydra, M., Patočka, J., Filip, M. (2023): Elemental profile identifies metallurgical pollution in epiphytic lichen *Xanthoria parietina* and (hypo)xanthine correlates with metals. – Science of The Total Environment 883: 163527.
- [26] Kularatne, K. I. A., de Freitas, C. R. (2013): Epiphytic lichens as biomonitors of airborne heavy metal pollution. – Environmental and Experimental Botany 88: 24-32.
- [27] Kumari, K., Kumar, V., Nayaka, S., Saxena, G., Sanyal, I. (2024): Physiological alterations and heavy metal accumulation in the transplanted lichen *Pyxine cocoes* (Sw.) Nyl. in Lucknow city, Uttar Pradesh. – Environmental Monitoring and Assessment 196: 84.
- [28] Li, M. N., Meng, J. W., Lin, D., Xu, P., Wang, L., Hu, Y. Q., Qin, C., Zhao, L. C., Xia, Y., Zhang, L. Y., Liu, H. J. (2024): Active biomonitoring of atmospheric element deposition in the heating period of Tangshan using *Ramalina sinensis*. – Polish Journal of Environmental Studies 33(5): 5767-5778.
- [29] Lin, D., Meng, J. W., Li, M. N., Wu, Q. F., Wang, L. P., Li, X. J., Song, J. J., Zhao, L. C., Xu, P., Xia, Y., Liu, H. J. (2024): Active biomonitoring of atmospheric element deposition

- using *Evernia mesomorpha* in Tangshan, China. – Applied Ecology and Environmental Research 22(2): 1191-1205.
- [30] Loppi, S., Paoli, L. (2015): Comparison of the trace element content in transplants of the lichen and in bulk atmospheric deposition: a case study from a low polluted environment (C Italy). – Biologia 70(4): 460-466.
- [31] Loppi, S., Ravera, S., Paoli, L. (2019): Coping with uncertainty in the assessment of atmospheric pollution with lichen transplants. – Environmental Forensics 20(3): 228-233.
- [32] Lucadamo, L., Corapi, A., Gallo, L. (2018): Evaluation of glyphosate drift and anthropogenic atmospheric trace elements contamination by means of lichen transplants in a southern Italian agricultural district. – Air Quality Atmosphere and Health 11(3): 325-339.
- [33] Malaspina, P., Giordani, P., Modenesi, P., Abemoschi, M. L., Magi, E., Soggia, F. (2014): Bioaccumulation capacity of two chemical varieties of the lichen *Pseudevernia furfuracea*. – Ecological Indicators 45: 605-610.
- [34] Massimi, L., Conti, M. E., Mele, G., Ristorini, M., Astolfi, M. L., Canepari, S. (2019): Lichen transplants as indicators of atmospheric element concentrations: a high spatial resolution comparison with PM10 samples in a polluted area (Central Italy). – Ecological Indicators 101: 759-769.
- [35] Osyczka, P., Boroń, P., Lenart-Boroń, A., Rola, K. (2018): Modifications in the structure of the lichen *Cladonia thallus* in the aftermath of habitat contamination and implications for its heavy-metal accumulation capacity. – Environmental Science and Pollution Research 25(2): 1950-1961.
- [36] Paoli, L., Winkler, A., Guttová, A., Sagnotti, L., Grassi, A., Lackovičová, A., Senko, D., Loppi, S. (2016): Magnetic properties and element concentrations in lichens exposed to airborne pollutants released during cement production. – Environmental Science and Pollution Research 24(3): 1-18.
- [37] Paoli, L., Vannini, A., Fačková, Z., Guarnieri, M., Bačkor, M., Loppi, S. (2018): One year of transplant: Is it enough for lichens to reflect the new atmospheric conditions? – Ecological Indicators 88: 495-502.
- [38] Reis, M. A., Alves, L. C., Freitas, M. C., Van Os, B., Wolterbeek, H. T. (1999): Lichens (*Parmelia sulcata*) time response model to environmental availability. – Science of The Total Environment 232: 105-115.
- [39] Sohrabi, M., Hassanzadeh, N., Hedayatzadeh, F., Mofid, M. (2021): Air quality and trace elements biomonitoring in Tehran urban areas using epiphytic lichen. – Iranian Journal of Health and Environment 13(4): 705-734.
- [40] Tumor, A., Abdulla, A., Abbas, A. (2011): Bio-monitoring of air quality in Urumqi city using lichens transplant method. – Environmental Pollution and Control 33(12): 1-8.
- [41] Vannini, A., Paoli, L., Nicolardi, V., Di Lella, L. A., Loppi, S. (2017): Seasonal variations in intracellular trace element content and physiological parameters in the lichen *Evernia prunastri* transplanted to an urban environment. – Acta Botanica Croatica 76(2): 171-176.

- [42] Will-Wolf, S., Jovan, S., Amacher, M. C. (2017): Lichen elements as pollution indicators: evaluation of methods for large monitoring programmes. – *The Lichenologist* 49(4): 415-424.
- [43] Wu, Y. Y., Gao, J., Zhang, G. Z., Zhao, R. K., Liu, A. Q., Sun, L. W., Li, X., Tang, H. L., Zhao, L. C., Guo, X. P., Liu, H. J. (2020): Two lichens differing in element concentrations have similar spatial patterns of element concentrations responding to road traffic and soil input. – *Scientific Reports* 10: 19001.
- [44] Zhao, L. L., Zhang, C., Jia, S. J., Liu, Q. X., Chen, Q. Z., Li, X., Liu, X. D., Wu, Q. F., Zhao, L. C., Liu, H. J. (2019): Element bioaccumulation in lichens transplanted along two roads: The source and integration time of elements. – *Ecological Indicators* 99: 101-107.
- [45] Zheng, X., Wu, Q. F., Wang, L. P., Liu, A. Q., Xu, C. Y., Li, X. J., Zhao, L. C., Xu, D., Meng, J. W., Liu, H. J. (2023): Composite samples with a small sample size reflect mean element concentrations in three lichens differing in element-specific concentrations. – *Applied Ecology and Environmental Research* 21(1): 609-622.

APPENDIX

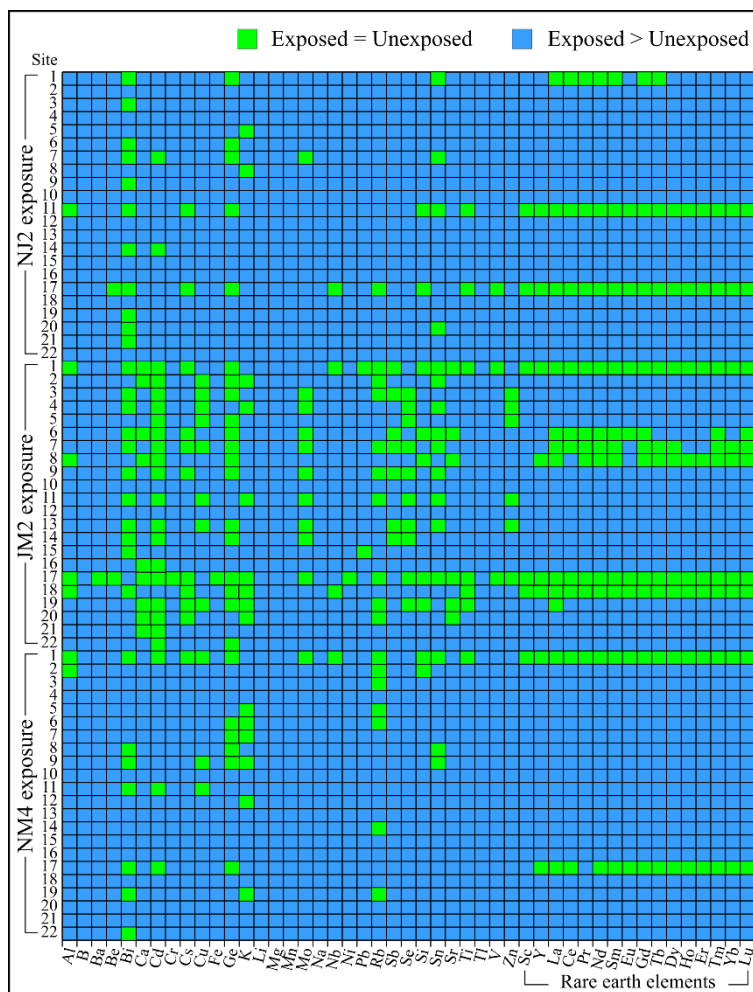


Figure S1. Differences between exposed and unexposed concentrations in *Ramalina sinensis* at each site in the NJ2, JM2 and NM4 exposures. NJ2 denotes exposure time of Nov. 2016 to Jan. 2017. JM2 denotes exposure time of Jan. to Mar. 2017. NM4 denotes exposure time of Nov. 2016 to Mar. 2017. Difference significance was tested using an independent samples T test. $n = 5$ for unexposed concentration. $n = 3$ for exposed concentrations

Table S1. Five-class interpretative scale for lichen transplants in different exposure time spans. EU ratio denotes exposed to unexposed ratio

ID	Bioaccumulation Class Description (Abbreviation)	EU ratio		
		4 weeks	8 weeks	12 weeks
1	Absence of bioaccumulation (A)	≤ 1.0	≤ 1.0	≤ 1.0
2	Low bioaccumulation (L)	(1.0, 1.8]	(1.0, 1.9]	(1.0, 1.8]
3	Moderate bioaccumulation (M)	(1.8, 2.5]	(1.9, 2.7]	(1.8, 3.1]
4	High bioaccumulation (H)	(2.5, 2.8]	(2.7, 3.5]	(3.1, 3.7]
5	Severe bioaccumulation (S)	> 2.8	> 3.5	> 3.7

Data were from Cecconi et al. (2019)

Table S2. Exposed concentrations of 47 elements in NJ2 exposure in *Ramalina sinensis*

	Norm.	Mean ($\mu\text{g}\cdot\text{g}^{-1}$)	CV (%)	Median ($\mu\text{g}\cdot\text{g}^{-1}$)	CV' (%)	Min. ($\mu\text{g}\cdot\text{g}^{-1}$)	Max. ($\mu\text{g}\cdot\text{g}^{-1}$)
Al*	N	2675	25.84	2604	33.54	1511	4307
B*	Non	10.22	32.27	9.144	34.95	6.245	20.69
Ba*	N	24.36	19.90	23.86	22.79	12.75	37.06
Be*	N	0.072	21.48	0.072	21.78	0.036	0.107
Bi*	N	0.109	18.90	0.107	17.81	0.063	0.155
Ca*	LN	3973	30.81	3700	33.19	1997	8252
Cd*	Non	0.305	31.62	0.281	23.58	0.164	0.531
Cr*	N	5.283	19.23	5.229	21.63	3.004	7.421
Cs*	N	0.323	19.22	0.323	20.85	0.183	0.458
Cu*	N	6.880	16.44	6.745	21.97	4.765	9.840
Fe*	N	1808	23.29	1780	21.38	970.0	3004
Ge*	N	0.210	19.22	0.209	18.49	0.127	0.290
K*	N	4136	15.11	4055	12.08	3036	5964
Li*	LN	1.535	24.72	1.473	21.23	0.877	2.733
Mg*	N	1178	24.17	1093	22.58	678.9	2052
Mn*	N	71.51	27.23	68.19	26.73	38.32	127.0
Mo*	N	0.265	21.44	0.262	24.96	0.167	0.422
Na*	LN	808.1	42.29	758.1	43.65	339.7	1793
Nb*	N	0.171	20.04	0.169	17.33	0.095	0.253
Ni*	N	2.321	20.42	2.291	17.90	1.360	3.446
Pb*	N	6.064	21.88	5.870	21.18	3.572	9.548
Rb*	Non	5.962	26.65	5.656	13.97	3.039	11.77
Sb*	N	0.239	22.30	0.242	25.83	0.142	0.370
Se*	N	0.535	15.36	0.526	17.65	0.388	0.720
Si*	N	6963	21.02	6658	24.45	4210	10467
Sn*	N	0.346	16.96	0.346	16.34	0.231	0.489
Sr*	N	12.72	22.01	12.28	22.74	7.900	20.87
Ti*	N	101.5	18.79	101.2	18.19	54.22	139.6
Tl*	N	0.085	21.97	0.082	22.56	0.053	0.131
V*	N	3.932	22.47	3.898	22.40	1.953	6.214
Zn*	Non	76.28	39.18	67.38	37.89	36.41	160.5
Rare earth elements							
Sc*	N	0.484	20.17	0.493	17.54	0.257	0.712
Y*	N	0.942	18.67	0.926	18.54	0.544	1.320
La*	N	1.570	20.20	1.550	22.07	0.887	2.215
Ce*	N	3.017	20.47	2.990	22.26	1.711	4.565
Pr*	N	0.339	20.52	0.339	22.03	0.196	0.516
Nd*	N	1.316	20.22	1.297	22.03	0.753	1.964
Sm*	N	0.249	19.90	0.247	21.78	0.135	0.357
Eu*	N	0.055	19.95	0.054	21.18	0.030	0.078
Gd*	N	0.217	20.09	0.215	21.19	0.120	0.317
Tb*	N	0.030	19.56	0.030	20.06	0.017	0.043
Dy*	N	0.172	19.07	0.169	19.74	0.099	0.245
Ho*	N	0.033	18.81	0.032	18.83	0.019	0.047

	Norm.	Mean ($\mu\text{g}\cdot\text{g}^{-1}$)	CV (%)	Median ($\mu\text{g}\cdot\text{g}^{-1}$)	CV' (%)	Min. ($\mu\text{g}\cdot\text{g}^{-1}$)	Max. ($\mu\text{g}\cdot\text{g}^{-1}$)
Er*	N	0.091	18.85	0.089	19.50	0.053	0.132
Tm*	N	0.013	18.70	0.013	22.12	0.007	0.018
Yb*	N	0.081	18.55	0.081	18.50	0.047	0.116
Lu*	N	0.012	19.14	0.011	21.87	0.007	0.017

NJ2 denotes exposure time of Nov. 2016 to Jan. 2017. "*" following an element indicates that the exposed concentration for the element was significantly higher than the unexposed concentration, otherwise no significant difference was found between the exposure and unexposed concentrations. In Norm. column, "N" indicates normal distribution; "Non" indicates no normal distribution. "LN" indicates log-normal distribution. "Min." denotes minimum value. "Max." denotes maximum value. "CV" denotes coefficient of variance calculated by (Eq.6). "CV'" denotes robust coefficient of variance calculated by (Eq.7). For elements with exposed concentrations following normal or log-normal distribution, an independent samples T test was conducted to test difference between the unexposed and exposed concentrations, otherwise a Mann-Whitney U test was conducted. For each element, n = 5 for unexposed concentration, n = 22 for exposed concentration

Table S3. Exposed concentrations of 47 elements in JM2 exposure in *Ramalina sinensis*

	Norm.	Mean ($\mu\text{g}\cdot\text{g}^{-1}$)	CV (%)	Median ($\mu\text{g}\cdot\text{g}^{-1}$)	CV' (%)	Min. ($\mu\text{g}\cdot\text{g}^{-1}$)	Max. ($\mu\text{g}\cdot\text{g}^{-1}$)
Al*	N	1881	17.11	1899	20.08	1320	2541
B*	N	10.66	16.70	10.57	20.00	7.391	14.66
Ba*	Non	17.23	29.15	17.31	21.20	9.780	36.89
Be*	N	0.053	14.30	0.053	14.50	0.035	0.069
Bi	N	0.108	25.13	0.106	27.85	0.070	0.183
Ca*	Non	1618	44.00	1402	37.86	760.9	3404
Cd	Non	0.145	19.13	0.142	17.65	0.104	0.218
Cr*	N	3.737	18.65	3.741	16.60	2.255	6.015
Cs*	N	0.256	14.17	0.253	17.97	0.198	0.333
Cu*	Non	5.610	17.10	5.306	15.96	4.036	8.039
Fe*	N	1213	15.35	1198	14.95	814.3	1560
Ge*	N	0.160	12.36	0.159	12.59	0.126	0.215
K*	LN	3706	15.59	3665	13.65	2717	5296
Li*	N	1.075	15.12	1.073	17.30	0.779	1.426
Mg*	N	702.5	13.93	697.9	15.14	502.7	885.4
Mn*	N	42.54	14.20	42.20	13.07	28.59	55.14
Mo*	N	0.184	16.53	0.180	19.22	0.133	0.268
Na*	N	342.8	19.73	339.8	16.61	213.6	515.9
Nb*	N	0.146	14.54	0.145	15.08	0.105	0.200
Ni*	N	1.630	18.33	1.582	19.28	1.050	2.446
Pb*	N	3.575	16.07	3.450	17.95	2.537	4.946
Rb*	N	4.661	14.09	4.680	12.89	3.026	6.290
Sb*	N	0.123	17.92	0.124	20.59	0.083	0.168
Se*	N	0.383	12.48	0.377	14.14	0.291	0.476
Si*	N	5200	16.35	5113	18.03	3590	7137
Sn*	N	0.294	18.62	0.299	22.44	0.183	0.411
Sr*	N	7.021	21.07	7.106	24.85	4.536	10.17
Ti*	N	82.95	14.31	82.39	18.71	58.83	105.5
Tl*	N	0.053	14.29	0.052	14.57	0.040	0.073
V*	N	2.733	13.60	2.713	13.25	1.889	3.541
Zn*	Non	30.61	24.05	28.76	21.96	20.52	54.27
Rare earth elements							
Sc*	N	0.413	15.43	0.408	14.64	0.286	0.579
Y*	N	0.770	14.54	0.751	16.15	0.561	1.029
La*	LN	1.250	14.81	1.234	17.83	0.925	1.631
Ce*	N	2.445	14.35	2.421	17.55	1.811	3.170
Pr*	N	0.281	14.12	0.278	16.15	0.206	0.362
Nd*	N	1.089	13.57	1.085	15.62	0.790	1.378
Sm*	N	0.204	14.26	0.198	15.36	0.143	0.262
Eu*	N	0.044	13.61	0.043	15.44	0.032	0.057
Gd*	N	0.181	14.63	0.178	14.51	0.124	0.236
Tb*	N	0.025	14.69	0.025	15.98	0.018	0.034
Dy*	N	0.144	14.83	0.141	16.70	0.100	0.189
Ho*	N	0.027	14.14	0.027	18.22	0.019	0.035

	Norm.	Mean ($\mu\text{g}\cdot\text{g}^{-1}$)	CV (%)	Median ($\mu\text{g}\cdot\text{g}^{-1}$)	CV' (%)	Min. ($\mu\text{g}\cdot\text{g}^{-1}$)	Max. ($\mu\text{g}\cdot\text{g}^{-1}$)
Er*	N	0.075	13.77	0.074	16.55	0.054	0.097
Tm*	N	0.011	13.78	0.010	16.33	0.007	0.013
Yb*	N	0.067	13.43	0.066	17.28	0.048	0.085
Lu*	N	0.012	13.12	0.009	15.70	0.007	0.012

JM2 denotes exposure time of Jan. to Mar. 2017. “*” following an element indicates that the exposed concentration for the element was significantly higher than the background concentration, otherwise no significant difference was found between the exposure and unexposed concentrations. In Norm. column, “N” indicates normal distribution; “Non” indicates no normal distribution. “LN” indicates log-normal distribution. “Min.” denotes minimum value. “Max.” denotes maximum value. “CV” denotes coefficient of variance calculated by (Eq.6). “CV’” denotes robust coefficient of variance calculated by (Eq.7). For elements with exposed concentrations following normal or log-normal distribution, an independent samples T test was conducted to test difference between unexposed and exposed concentrations, otherwise a Mann-Whitney U test was conducted. For each element, n = 5 for unexposed concentration; n = 22 for exposed concentration

Table S4. Exposed concentrations of 47 elements in NM4 exposure in *Ramalina sinensis*

NM4	Norm.	Mean ($\mu\text{g}\cdot\text{g}^{-1}$)	CV (%)	Median ($\mu\text{g}\cdot\text{g}^{-1}$)	CV' (%)	Min. ($\mu\text{g}\cdot\text{g}^{-1}$)	Max. ($\mu\text{g}\cdot\text{g}^{-1}$)
Al*	N	2287	25.68	2157	22.84	1278	4027
B*	Non	13.97	28.13	13.65	16.34	7.671	29.55
Ba*	Non	25.69	28.91	23.71	21.28	14.94	51.64
Be*	Non	0.072	24.20	0.068	21.37	0.048	0.126
Bi*	N	0.127	22.41	0.123	16.28	0.070	0.206
Ca*	Non	3812	29.75	3653	22.74	2167	8155
Cd*	LN	0.298	41.69	0.267	35.45	0.137	0.698
Cr*	Non	5.398	24.81	5.074	21.18	3.495	10.00
Cs*	Non	0.342	21.95	0.324	19.28	0.227	0.538
Cu*	LN	6.756	20.26	6.723	15.79	4.437	10.84
Fe*	LN	1841	22.59	1752	24.97	1232	2991
Ge*	Non	0.218	23.04	0.209	20.32	0.147	0.373
K*	N	3822	13.19	3789	17.23	2830	4851
Li*	N	1.715	22.85	1.666	21.46	0.978	2.939
Mg*	Non	1181	28.42	1105	20.99	726.4	2187
Mn*	Non	70.73	29.76	64.80	26.11	44.17	135.9
Mo*	Non	0.271	27.60	0.255	21.82	0.178	0.567
Na*	Non	867.48	53.40	708.3	36.61	381.3	2376
Nb*	LN	0.187	20.73	0.179	18.86	0.119	0.313
Ni*	Non	2.369	25.53	2.320	21.16	1.431	4.219
Pb*	N	6.391	18.46	6.335	15.25	3.774	9.331
Rb*	N	5.685	19.79	5.469	23.03	3.877	8.456
Sb*	N	0.234	25.68	0.228	28.80	0.135	0.426
Se*	Non	0.519	20.11	0.502	18.09	0.366	0.891
Si*	N	7113	27.34	6929	22.55	3584	12978
Sn*	N	0.358	13.97	0.358	14.77	0.256	0.459
Sr*	Non	12.95	24.31	12.48	16.89	7.190	22.97
Ti*	Non	104.2	21.25	98.35	19.08	71.85	175.0
Tl*	N	0.093	24.75	0.090	24.78	0.054	0.162
V*	Non	3.908	25.32	3.617	22.42	2.651	7.241
Zn*	Non	68.31	41.77	59.86	36.83	37.26	156.3
Rare earth elements							
Sc*	Non	0.499	21.27	0.475	21.64	0.328	0.775
Y*	Non	0.983	21.32	0.918	23.18	0.653	1.598
La*	Non	1.647	21.73	1.576	22.34	1.091	2.625
Ce*	Non	3.247	22.36	3.067	23.66	2.116	5.140
Pr*	LN	0.367	22.15	0.345	22.03	0.239	0.585
Nd*	Non	1.423	22.48	1.346	21.20	0.934	2.288
Sm*	Non	0.259	23.62	0.240	25.35	0.174	0.431
Eu*	Non	0.056	22.67	0.054	21.48	0.038	0.096
Gd*	Non	0.225	23.09	0.212	21.34	0.150	0.385
Tb*	Non	0.032	22.49	0.030	23.53	0.021	0.052
Dy*	Non	0.181	22.77	0.168	22.84	0.119	0.300
Ho*	Non	0.034	22.72	0.032	22.63	0.023	0.057

NM4	Norm.	Mean ($\mu\text{g}\cdot\text{g}^{-1}$)	CV (%)	Median ($\mu\text{g}\cdot\text{g}^{-1}$)	CV' (%)	Min. ($\mu\text{g}\cdot\text{g}^{-1}$)	Max. ($\mu\text{g}\cdot\text{g}^{-1}$)
Er*	Non	0.096	22.27	0.090	20.63	0.064	0.158
Tm*	Non	0.013	23.52	0.012	21.51	0.009	0.023
Yb*	Non	0.084	22.38	0.078	22.82	0.057	0.141
Lu*	Non	0.012	23.27	0.011	23.74	0.008	0.021

NM4 denotes exposure time of Nov. 2016 to Mar. 2017. "*" following an element indicates that the exposed concentration for the element was significantly higher than the unexposed concentration, otherwise no significant difference was found between the exposed and unexposed concentrations. In Norm. column, "N" indicates normal distribution; "Non" indicates no normal distribution. "LN" indicates log-normal distribution. "Min." denotes minimum value. "Max." denotes maximum value. "CV" denotes coefficient of variance calculated by (Eq.6). "CV'" denotes robust coefficient of variance calculated by (Eq.7). For elements with exposed concentrations following normal or log-normal distribution, an independent samples T test was conducted to test difference between the unexposed and exposed concentrations, otherwise a Mann-Whitney U test was conducted. For each element, n = 5 for unexposed concentration; n = 22 for exposed concentration. Part of the data were published in Li et al. (2024)

Table S5. ANOVA and Kruskal - Wallis results

Elements	Kruskal-Wallis test		One-way ANOVA	
	H(2)	p	F(2, 63)	p
B*	19.67	0.00	11.52	0.00
K*	8.50	0.01	4.44	0.02
Bi*	7.23	0.03	3.87	0.03
Cd*	39.98	0.00	42.12	0.00
Al*	17.66	0.00	12.27	0.00
Ba	28.89	0.00	19.66	0.00
Be*	26.69	0.00	16.16	0.00
Ca*	37.92	0.00	61.39	0.00
Cr*	30.97	0.00	24.14	0.00
Cs*	24.03	0.00	15.88	0.00
Cu	16.63	0.00	10.56	0.00
Fe*	35.92	0.00	31.07	0.00
Ge*	29.51	0.00	19.49	0.00
Li*	36.89	0.00	32.55	0.00
Na*	40.24	0.00	38.36	0.00
Mg	41.05	0.00	43.68	0.00
Mn*	40.07	0.00	35.91	0.00
Mo	32.02	0.00	25.42	0.00
Nb*	20.47	0.00	11.29	0.00
Ni*	28.87	0.00	23.12	0.00
Pb*	41.76	0.00	71.72	0.00
Rb	18.66	0.00	9.39	0.00
Sb*	42.78	0.00	68.04	0.00
Se	36.69	0.00	35.67	0.00
Si*	21.90	0.00	13.32	0.00
Sn*	14.60	0.00	10.57	0.00
Sr*	41.60	0.00	59.60	0.00
Ti*	19.08	0.00	10.95	0.00
Tl*	40.66	0.00	50.19	0.00
V	32.59	0.00	23.19	0.00
Zn	42.03	0.00	51.16	0.00
REE*	18.39	0.00	10.99	0.00
PLI _{site} *	40.22	0.00	40.92	0.00
Sc*	12.41	0.00	6.44	0.00
Y*	19.49	0.00	12.08	0.00
La*	20.40	0.00	14.08	0.00
Ce*	20.47	0.00	13.54	0.00
Pr*	18.51	0.00	12.07	0.00
Nd*	19.22	0.00	12.12	0.00
Sm*	16.81	0.00	9.88	0.00
Eu*	20.60	0.00	12.59	0.00
Gd	14.56	0.00	8.28	0.00
Tb*	15.67	0.00	9.28	0.00

Elements	Kruskal-Wallis test		One-way ANOVA	
	H(2)	p	F(2, 63)	p
Dy*	16.23	0.00	9.44	0.00
Ho*	17.72	0.00	10.61	0.00
Er*	19.60	0.00	11.80	0.00
Tm	20.79	0.00	11.71	0.00
Yb*	18.76	0.00	11.10	0.00
Lu	17.96	0.00	10.40	0.00

Elements with a “*” denote that the data follow a normal/log - normal distribution, and thus the ANOVA results are applicable; otherwise, the data do not follow a normal distribution, and the Kruskal - Wallis results are applicable. In H(2), H represents the test statistic of the Kruskal - Wallis test, and the number 2 within the parentheses indicates the degrees of freedom; p is the significance level of the Kruskal - Wallis test. In F(2, 63), F represents the test statistic of the One - way ANOVA, the numbers 2 and 63 within the parentheses denote the degrees of freedom between groups and within groups, respectively; p is the significance level of the One - way ANOVA